Effect of Dissolved Hydrogen on Crack Growth Rate in Stainless Steel

K.J. Choi, S.C. Yoo, T.H. Kim, S.H. Kim, and J.H. Kim*
Ulsan National Institute of Science and Technology (UNIST), School of Mechanical and Nuclear Engineering,
Republic of Korea
Corresponding author: kimjh@uinst.ac.kr

ABSTRACT

Irradiation-assisted stress corrosion cracking has affected reactor core internal structures fabricated from austenitic stainless steels in pressurized water power plants. The general failure pattern of such cracking indicates that, as nuclear plan

ts age and neutron fluence increases, austenitic stainless steels can become susceptible to intergranular failure. Of the observed types of radiation damage, it has been shown that radiation-induced segregation, second-phase hardening, and radiation-induced hardening increased the susceptibility to intergranular stress corrosion cracking, which generally occurs at doses between 0.5 dpa (for boiling water reactors) and 2–3 dpa (for pressurized water reactors). Recently, domestic nuclear power plants (NPPs) arrived at a state of long-term operation, and some of these plants have been irradiated with more than 3 dpa. Thus, the affected NPPs were exposed to the risk of irradiation-assisted stress corrosion cracking. Furthermore, there has been a recent trend to increase dissolved hydrogen in the primary section of pressurized water power plants up to approximately 50 cc/kg dissolved hydrogen (DH), in order to reduce susceptibility to stress corrosion cracking in Ni base alloy. However, increasing DH to this level may detract from the resistance to cracking in stainless steel. To address this issue, the final objective of the present study is to evaluate the integrity of internal structures by investigating the characteristics of irradiation-assisted stress corrosion cracking and determining a relationship between dissolved hydrogen and environmental factors, the stress intensity factor K, and crack growth rate. In particular, this study focuses on the relationship between stress corrosion crack growth and DH in as-received austenitic stainless steel based on crack growth measurement. The results show that increasing DH makes crack growth more active by arresting the phase transition of Ni/NiO or Fe2O3/Fe3O4, and a peak in crack growth rate exists near the transition.

1. Introduction

In recent years, domestic nuclear power plants (NPPs) have reached long-term operation status, and half of all NPPs have been operating for more than 20 years. Moreover, some of these plants have been irradiated with more than 3 displacements per atom (dpa). Because irradiation-assisted stress corrosion cracking (IASCC) typically occurs at doses between 0.5 dpa (for boiling water reactors, BWRs) and 2–3 dpa (for pressurized water reactors, PWRs) [1], it can be expected that many NPPs are exposed to the risk of IASCC. In countries outside Korea, this risk has been shown to increase steadily.

The general failure pattern of IASCC indicates that, as nuclear plants age and neutron fluence increases, various austenitic stainless steels become susceptible to intergranular failure. Irradiation produces defects, and defect clusters in grains alter dislocation and dislocation loop structures and produce defect–impurity and defect–cluster–impurity complexes, leading to radiation-induced hardening. Irradiation also leads to changes in the stability of second-phase precipitates and to the local alloy chemistry near grain boundaries, precipitates, and defect clusters. Grain boundary microchemistry that differs significantly from bulk composition can be produced in association with both radiation-induced segregation and thermally driven segregation of alloying and impurity elements [2]. Of these various radiation damages, it has been shown that radiation-induced segregation, second-phase hardening, and radiation-induced hardening can make steels more susceptible to intergranular stress corrosion cracking (IGSCC).

Of the internal structural parts of PWRs, baffle-former bolts (which assemble formers and baffles) exhibit relatively high susceptibility to irradiation-assisted stress corrosion cracking due to tensile stress occurring after the assembly of the formers and baffles. In other words, baffle-former bolts consisting of austenitic stainless steel are susceptible to IASCC due to doses greater than 3 dpa and the tensile stress formed during assembly.

Recently, dissolved hydrogen (DH) has been suggested as an important factor in the stress corrosion cracking of Ni base alloy. Therefore, to reduce the susceptibility of such alloys to stress corrosion cracking, there has been a tendency to increase DH of the primary section of pressurized water power plants up to approximately 50 cc/kg. However, the electrochemical corrosion potential (EcP) under these conditions is further from the EcP of the Ni/NiO phase transition than that at 25 cc/kg DH based on the results of a previous study, which showed that the peak stress corrosion rates occurring at the phase transition tend to decrease symmetrically as delta EcP values move away from the Ni/NiO phase transition [3, 4].

Although the level of 50 cc/kg DH can reduce susceptibility to stress corrosion cracking in Ni base alloy, it may aggravate the resistance to cracking in stainless steel. In a previous study [5] that investigated the effects of DH (0–30 cc/kg) on stress corrosion cracking of irradiated stainless steel by performing a slow strain rate test, it was concluded that the %IGSCC increased with increasing DH. Moreover, the corrosion products on the surface of fractured grain boundaries tended to increase in size as DH increased. In fact, the effect of DH on the IGSCC behavior of irradiated stainless steel was similar to that of Alloy 600. However, it remains difficult to evaluate the acceleration mechanism induced by increased DH because there are insufficient data available in the literature regarding the influence of DH on IGSCC susceptibility in austenitic stainless steel.

To address this lack of knowledge, further tests must be performed to understand the effects of DH on irradiation-assisted stress corrosion crack growth in stainless steel in a primary water environment. Additionally, further understanding of the processes active at the level of 50 cc/kg DH are required to evaluate the integrity of steel. The present study investigated primarily the relationship between stress corrosion crack growth and DH in as-received austenitic stainless steel based on crack growth measurement. In future, with stainless steel simulating irradiation damage (such as radiation-induced segregation, second-phase hardening, and radiation-induced hardening), the investigation of the effects of DH will be conducted by comparing our results with those for as-received stainless steel.

2. Experimental Procedure

To evaluate the relationship between IASCC growth and DH in terms of crack growth measurements, a plate of austenitic stainless steel (Type 316L) was used; its composition is presented in Table I. Figure 1 illustrates the direction of the warm rolling process,
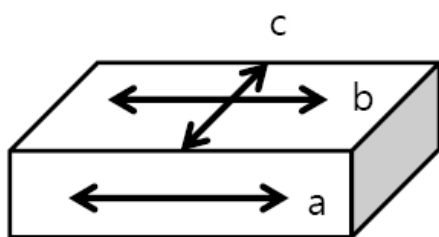
which simulates radiation damage such as radiation-induced segregation, second-phase hardening, and radiation-induced hardening. For the simulation, which was conducted at 250℃, 10% of warm rolling was conducted in the 'a' direction (first step), followed by 5% of warm rolling in the 'b' and 'c' directions (section step). After warm rolling, heat treatment was performed at 630℃ for 100 h to form carbide precipitates and complete the simulation of the radiation damage. Additionally, at 250℃, 20% of warm rolling was conducted in the 'a' direction (first step) and then in the 'b' and 'c' directions (second step), followed by 30% of warm rolling in the 'a' direction (third step). After warm rolling, the heat treatment described above was applied to form carbide precipitates. Based on these steps, the matrix of the warm rolling for the radiation damage simulation consists of 3 conditions: as-received, 10–5–5%, and 50–20–20% warm rolled samples. Material for test specimens was extracted from the samples for microstructure analysis and crack growth measurement. In this study, it was decided to investigate the relationship between stress corrosion crack growth and DH in as-received austenitic stainless steel.

The procedure of crack growth measurement was determined following previous studies [6-10]. The 0.5T compact tension (CT) specimens used in this study were machined with 5% side grooves on each side and instrumented with platinum current and potential probe leads for direct current (DC) potential drop measurements of crack length. Current flow through the sample was reversed about once per second, primarily to reduce measurement errors associated with thermocouple effects and amplifier offsets. Zirconia sleeves and washers were used to electrically insulate the CT specimens from the loading pins and grips. The relationship between crack length and voltage was determined according to the method of Hicks and Pickard (described in ASTM E647).

Before the experiment, pre-cracking was performed; this process produces intergranular cracks similar to those formed by irradiation-assisted stress corrosion cracking. The pre-cracking was performed at a frequency of 10 Hz and a load ratio of K_{min} to K_{max} (R) 0.1 and sine waveform in air condition and K_{max} was determined based on ASTM E647.

Next, at a frequency of 1 Hz for R values of 0.3, 0.5, and 0.7, the experiment was performed at a lower K_{max} than that at which the crack growth measurement was performed. Subsequently, pre-cracking was executed at

Fig. 1. Direction of warm rolling for simulation of radiation damage

Table I. Chemical composition and material properties of Type 316L stainless steel

Chemical composition (wt.%)												Tensile Test (MPa)	
C	Si	Mn	P	S	Cr	Ni	Cu	Al	Ti	N	Mo	Y.S.	T.S
0.016	0.49	1.38	0.033	0.002	16.6	10	0.13			0.09	2.02	276	590

Table II. Procedures for crack growth measurement

| Step	R	Waveform	Frequency (Hz)	Hold (s)	K_{max} (MPa√m)
0	0.1	Sine	10		
1	0.3	Sine	1		16
2	0.5	Sine	1		18
3	0.7	Sine	1		20
4	0.7	Sine	0.1		20
5	0.7	Sine	0.01		20
6	0.7	Triangle	0.001		30
7	0.7	Trapezoidal	0.001	9,000	30
8	1	Constant	DH=25 cc/kg		30
7	0.7	Trapezoidal	0.001	9,000	30
8	1	Constant	DH=50 cc/kg		30
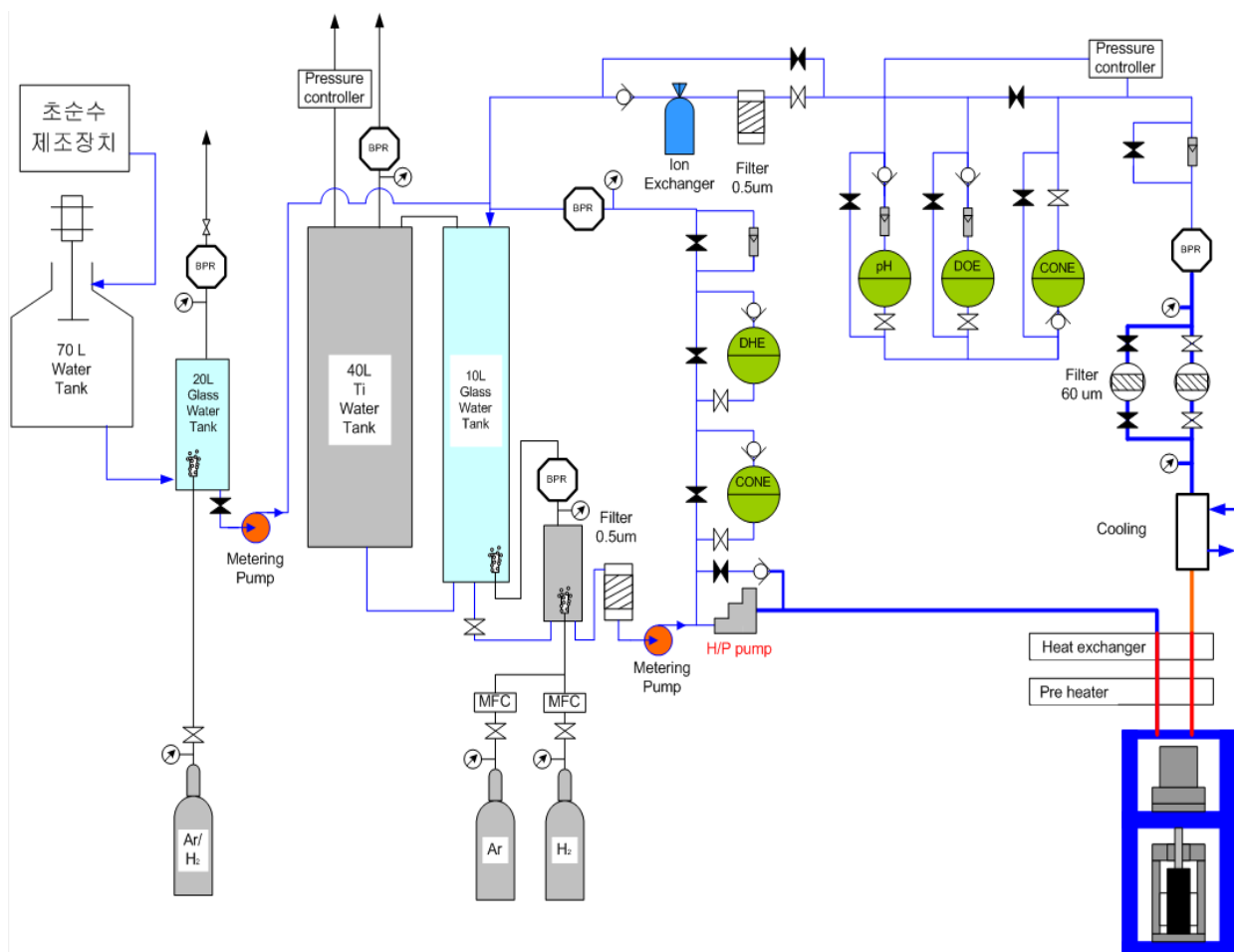
Fig. 2. Schematic of crack growth measurement

R = 0.7 and frequencies of 0.1 and 0.01 Hz. Finally, the pre-cracking was completed at a frequency of 0.001 Hz, for R = 0.7, with triangle (step 6) and trapezoidal (step 7) waveforms. These processes are described in Table II. In particular, at K = 30 MPa√m (i.e., constant loading), the crack growth rate was measured at 25 and 50 cc/kg DH.

Tests were conducted in an autoclave system specially constructed for the present study. Careful consideration was given to ensuring extremely rigorous chemistry control, and near-theoretical water conductivity was achieved routinely. In addition to the autoclave system, a special suite of software was written to control the overall system and facilitate the measurement of crack growth using the DC potential drop technique. Figure 2 presents a schematic of the autoclave system. The system is fully instrumented for oxygen, hydrogen, pH, and conductivity for both the

inlet and outlet water. Distilled and demineralized water is supplied to the makeup system from the laboratory water supply system. The makeup system then circulates the water through a demineralizer/filter system to ensure cleanliness. Makeup water is supplied through a chemistry conditioning system, where the water chemistry is adjusted, to the autoclave system. Provision has been made for injection of chemicals as well as for gas purging. In the present study, the effects of DH on the susceptibility to stress corrosion crack growth were evaluated by varying DH. The test was performed in a 3.79 L stainless steel autoclave, which can maintain conditions of 1200 ppm B, 2 ppm Li, 25 and 50 cc/kg DH, DO < 10 ppb, 340°C, and 17.5 MPa.
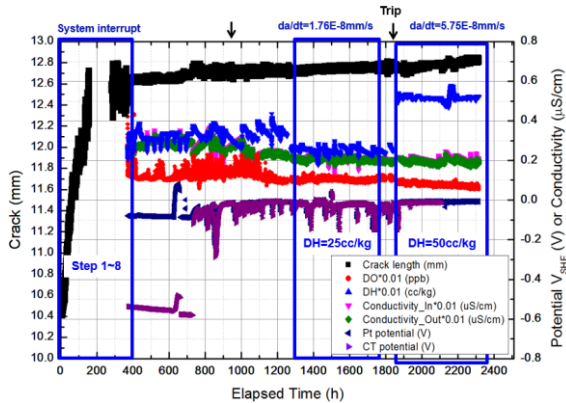
(a) Total test sequence
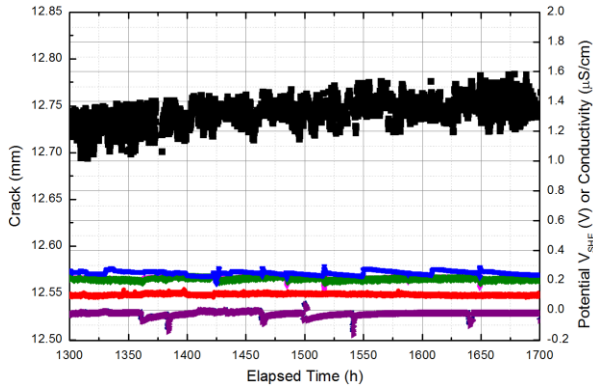
(b) Magnified view at 25cc/kg DH sequence
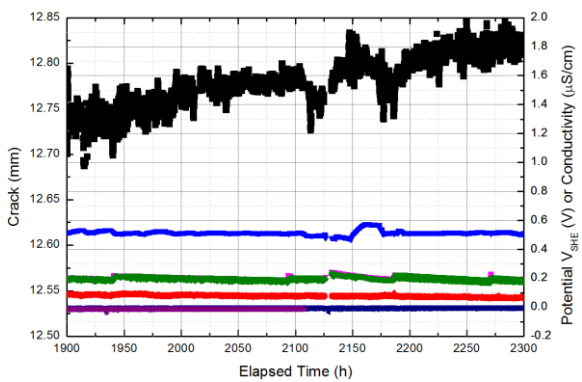
(c) Magnified view at 50cc/kg DH sequence

Fig. 3. Details of as-received stainless steel test results
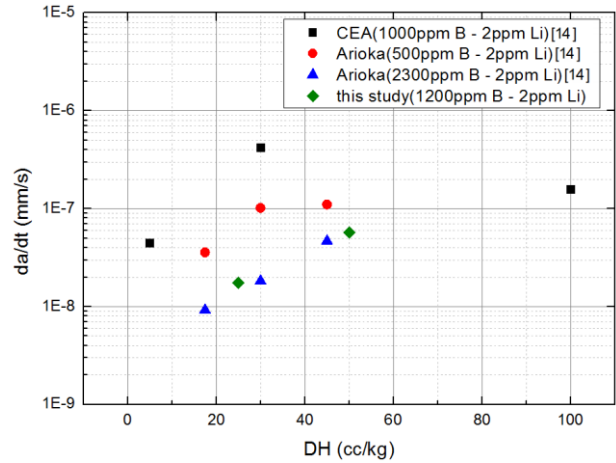

Fig. 5. Distribution of crack growth rate with DH

Provision has been made for injection of chemicals as well as for gas purging. In the present study, the effects of DH on the susceptibility to stress corrosion crack growth were evaluated by varying DH. The test was performed in a 3.79 L stainless steel autoclave, which can maintain conditions of 1200 ppm B, 2 ppm Li, 25 and 50 cc/kg DH, DO < 10 ppb, 340°C, and 17.5 MPa.

3. Results and Discussion

Figure 3(a) illustrates the results of the crack growth measurement that was performed for as-received austenitic stainless steel Type 316L under test conditions simulating the primary section in a PWR. The total elapsed time was 2325 h and the stabilization of water conditions was conducted after pre-cracking was performed for 420 h.

At DH 25 cc/kg (Fig. 3(b)), the crack growth rate was found to be about 1.76E-8 mm/s, estimated in the region from 1279 h to 1750 h. Conversely, at DH 50 cc/kg (Fig. 3(c)), the growth rate was found to be about 5.75E-8 mm/s, estimated in the region from 1878 h to 2325 h. The green diamond-shaped in Fig. 4 denote the results of the present study, indicating that the results presented here are within the range expected based on previous studies (1E-8–1E-6 mm/s). Thus, this figure corresponds to the tendency shown in previous studies for crack growth rates to increase with stress intensity [11-13].

Figure 5 illustrates the distribution of crack growth rate with DH for both the present study and a previous study [14], demonstrating the effect of DH on stress corrosion crack growth. Based on this figure, it is clear that increasing DH accelerates the growth rate, as was shown in the previous study [14]. Additionally, based on the distribution of the growth rates, it can be assumed that a peak in crack growth rates may exist between 40 cc/kg and 100 cc/kg. This distribution may be similar to that observed for Ni base alloy, in which crack growth rates tend to decrease symmetrically as DH values move away from the Ni/NiO phase

transition. It may be possible to explain this scenario based on a Pourbaix diagram.

A previous study [14] observed that EcP of SS316LN is -0.685 V at 25cc/kg DH (red squares in Fig. 6) and -0.719 V at 80cc/kg DH (blue circles in Fig. 6) at 310℃, and it seems that EcP values vary within the pink shaded box shown in the figure under the typical PWR environment. Within this pink box, it appears that a peak in the crack growth rate exists among the phase transitions of Ni/NiO and Fe_2O_3/Fe_3O_4. These phase transitions are interfaces that determine the stable phase under any given conditions, and may improve or aggravate resistance to crack growth by affecting the oxide type, thickness, and structure on surfaces and grain boundaries. In fact, with increasing DH, the thickness of the oxide layer on the surface of Ni base alloy and stainless steel tends to decrease, but the thickness on the grain boundary near the surface tends to increase owing to thinning of the oxide layer on the surface [5, 14, 16-17]. In terms of the effects of DH on the thickness of the oxide layer, it seems that stainless steel experiences similar effects to Ni base alloy, such that changes induced by the increased DH affect the resistance to stress corrosion crack growth.

Finally, based on the above information, two hypotheses can be proposed regarding the acceleration mechanism caused by increased DH. The first is hydrogen embrittlement, which embrittles the grain boundary and can aggravate the resistance to stress corrosion crack growth. Increasing DH induces the thinning of the oxide layer on the surfaces of stainless steel and Ni base alloy by changing EcP. Thus, it would make stainless steel more susceptible to H embrittlement and result in increased crack growth. However, this hypothesis cannot clearly explain why the peak crack growth rates exist within 40 and 100 cc/kg DH (shown in Fig. 5). In contrast, this distribution is similar to that observed for Ni base alloy, in that the crack growth rates tend to decrease symmetrically as delta EcP values move away from the Ni/NiO phase transition. In fact, in the present study, it seems that crack growth rates tend to decrease symmetrically as delta EcP values move away from the phase transitions of both Ni/NiO and Fe_2O_3/Fe_3O_4. This suggests a similar acceleration method, although stainless steel has a different EcP to Ni base alloy, which could explain why the peak in crack growth rates exists at a different DH.

In future, to verify these hypotheses regarding the effects of DH on stress corrosion crack growth, it will be necessary to investigate at which phase transition the peak in crack growth rates appears, to determine how the transition affects the resistance to stress corrosion crack growth, and to identify the oxide film of stainless steel on the fractured surface.

4. Conclusions

To investigate the effects of dissolved hydrogen (DH) on the resistance to stress corrosion crack growth of austenitic stainless steel, crack growth measurement was performed at 25 cc/kg and 50 cc/kg DH. The DH increased the crack growth rates, and the growth rate at 25 cc/kg DH was lower than that at 50 cc/kg DH. However, this trend does not increase constantly, because the growth rate starts to decreases when DH exceeds a particular value. In particular, the results demonstrate that the peak in growth rates exists between 40 and 100 cc/kg DH. Phase transitions are interfaces that determine the stable phase under given conditions, and may improve or aggravate resistance to crack growth by affecting oxide type, thickness, and structure. In the present study, it appears that the peak occurs owing to the existence of the Ni/NiO or Fe_2O_3/Fe_3O_4 phase transitions that occur in the area of EcP under a typical PWR environment.

ACKNOWLEDGMENTS

REFERENCES

[1] K.E.Sickafus, E.A.Kotomin and B.P.Uberuaga, "Proceedings of the NATO Advanced Study Institute on Radiation Effects in Solids", Physics and Chemistry, Vol. 235, 2004

[2] H.M.Chung and W.J.Shack, "Irradiation Assisted Stress Corrosion Cracking Behavior of Austenitic Stainless Steels Applicable to LWR Core Internals", NUREG/CR-6892, ANL 04/10, 2006

[3] D.S.Morton, S.A.Attanasio and G.A.Young, "Primary Water SCC Understanding and Characterization Through Fundamental Testing in the Vicinitiy of the Nickel/Nickel Oxide Phase Transition", LM-01K038. 2001

[4] R.A. Etien, E.Richey, D.S.Morton, and J.Eager, "SCC Initiation Testing of Alloy 600 in High Temperature Water" 15th International Conference on Environmental Degradation, TMS, 2011

[5] G.Furutani, N.Nakajima, T.Konishi and M.Kodama, "Stress Corrosion Cracking on Irradiated 316 Stainless Steel", Journal of Nuclear Materials, Vol. 288, 2001

[6] J.H.Kim, R.G.Ballinger and P.W.Stahle, "SCC Crack Growth in 316L Weld Metals in BWR Environments", Nace - International Corrosion Conference Series, March 16-20, 2008

[7] J.H.Kim and R.G.Ballinger, "Stress Corrosion Cracking Crack Growth Behavior of Type 316L Stainless Steel Weld Metals in Boiling Water Reactor Environments", Corrosion, Vol. 64, 2008

[8] J.R.Hixon, J.H.Kim and R.G.Ballinger, "Effect of thermal aging on SCC and mechanical properties of stainless steel weld metals", 13th International Conference on

Environmental Degradation of Materials in Nuclear Power Systems 2007, Vol. 3, 2007

[9] P.L.Andresen, J.Hickling, A.Ahluwalia and J.Wilson, "Effects of Hydrogen on Stress Corrosion Crack Growth of Ni Alloys in High-Temperature Water", Corrosion, Vol. 64, 2008

[10] P.L.Andresen, "Environmental Assisted Growth Rate Response of Nonsensitized AISI 316 grade Stainless Steel in High Temperature Water", Corrosion Vol. 44, 1988

[11] C.Guerre, O.Raquet, E.Herms, M.L.Calvar and G.Turluer, "SCC Growth Behaviour of Austenitic Stainless Steel in PWR Primary Water Conditions", 12th International Conference on Environmental Degradation of Materials in Nuclear Power Systems-Water Reactors 2005

[12] P.L.Andressn, M.M.Morra and W.Catlin, "Effects of Si on SCC of Stainless Steel and Ni Alloys", ICG-EAC 2004

[13] T.Yamada, T.Terachi, G.Chiba and K.Arioka, "Crack Growth Behavior of Cold Worded SUS316 in Hydrogenated High Temperature Water" ICG-EAC 2005

[14] Q.Raquer, E/Herms, F.Vaillant and T.Couvant, "SCC of Cold-Worked Austenitic Stainless Steels in PWR Conditions", Advances in Materials Science, Vol. 7, 2007

[15] C.H.Jang, P.Y.Cho, H.Jang and J.D.Hong and I.S.Jeong, "The Effect of Material Variability and Dissolved Hydrogen on LCF Behavior of Stainless Steels in Simulated PWR Environment", ICG-EAC 2010

[16] T.Terachi, N.Totsuka, T.Yamada and T.Nakagawa, "Influence of Dissolved Hydrogen on Structure of Oxide Film on Alloy 600 Formed in Primary Water of Pressurized Water Reactors", Journal of Nuclear Science and Technology, Vol. 40, 2003

[17] K.Dozaki, D.Akutagawa, N.Nagata, H.Takiguchi and K.Norring, "Effects of Dissolved Hydrogen Content in PWR Primary Water on PWSCC Initiation Property", E-Journal of Advanced Maintenance, Vol. 2, 2010